Bulk nanobubbles from acoustically cavitated aqueous organic solvent mixtures

Nirmalkar, Neelkanth; Pacek, Andrzej; Barigou, Mostafa

DOI:
10.1021/acs.langmuir.8b03113

Document Version
Peer reviewed version

Citation for published version (Harvard):
Nirmalkar, N, Pacek, A & Barigou, M 2019, 'Bulk nanobubbles from acoustically cavitated aqueous organic solvent mixtures', *Langmuir*, vol. 35, no. 6, pp. 2188-2195. https://doi.org/10.1021/acs.langmuir.8b03113

Interface Components: Nanoparticles, Colloids, Emulsions, Surfactants, Proteins, Polymers

Bulk nanobubbles from acoustically cavitated aqueous organic solvent mixtures

Neelkanth Nirmalkar, A. W. Pacek, and Mostafa Barigou

Langmuir, **Just Accepted Manuscript** • DOI: 10.1021/acs.langmuir.8b03113 • Publication Date (Web): 12 Jan 2019

Bulk nanobubbles from acoustically cavitated aqueous organic solvent mixtures

N. Nirmalkar, A.W. Pacek, M. Barigou✉

School of Chemical Engineering, University of Birmingham, Edgbaston, Birmingham B15 2TT, United Kingdom

Abstract

We investigate the existence and stability of bulk nanobubbles in various aqueous organic solvent mixtures. Bulk nanobubble suspensions generated via acoustic cavitation are characterised in terms of their bubble size distribution, bubble number density and their zeta potential. We show that bulk nanobubbles exist in pure water, but do not exist in pure organic solvents and they disappear at some organic solvent-water ratio. We monitor the nanobubble suspensions over a period of a few months and propose interpretations for the differences behind their long-term stability in pure water versus their long-term stability in aqueous organic solvent solutions. Bulk nanobubbles in pure water are stabilised by their substantial surface charge arising from the adsorption of hydroxyl ions produced by self-ionisation of water. Pure organic solvents do not auto-ionise and, therefore, nanobubbles cannot exist in concentrated aqueous organic solvent solutions. Due to preferential adsorption of organic solvent molecules at the nanobubble interfaces, the surface charge of the nanobubbles decreases with solvent content, but the strong hydrogen bonding near their interfaces ensures their stability. The mean bubble size increases monotonically with solvent content whilst the surface tension of the mixture is sharply reduced. This is in agreement with literature results on macro and microbubbles in aqueous organic solutions, but it stands in stark contrast to the behaviour of macro and microbubbles in aqueous surfactant solutions.

✉Corresponding author; Email: m.barigou@bham.ac.uk

Introduction

Bulk nanobubbles are a new class of nanoscale bubble system. They exist in bulk liquid, they are spherical and exhibit long-term stability on a timescale of weeks or months.[1-3] Such extraordinary longevity exceeds by far the bubble lifetime on the scale of microseconds predicted by the classical Epstein and Plesset theory[4], challenging our understanding of bubble physics and behaviour. Given their high curvature and their high Laplace pressure, bubble dynamics theory suggests that such entities should not exist. Because of this conundrum, the use of the Young-Laplace equation at the nanoscale has been questioned, but recent results on surface nanobubbles based on molecular dynamics simulations[5] and electrochemical measurements[6] seem to support its plausibility. Despite a number of recent studies claiming the existence of bulk nanobubbles, this is still an emerging field and their existence is still not widely accepted.[7] When generating bulk nanobubbles in pure water, a question that often arises is whether such nano-entities are nanobubbles or solid nanoparticles which have detached from adjacent surfaces, or simply arising from impurities. Similarly, in mixtures of water and organic liquids, doubt exists as to whether the nano-entities observed are nanobubbles or supramolecular structures.[8,9]

Evidence of the existence of bulk nanobubbles has been reported in a number of studies using various production, visualisation and characterizing techniques including: nanobubbles generated via hydrodynamic cavitation and bubble size distribution measured by an ultrasound wave attenuation technique[10], by SEM based on a freeze-fracture replica method[2] and by TEM;[11] generation of nanobubbles via chemical reaction and characterised using Cryo-EM[12]; nanobubbles generated spontaneously in aqueous NaCl solutions and analysed using DLS;[13] generation of nanobubbles by acoustic cavitation and characterised by a nanoparticle tracking technique and DLS;[14] generation of nanobubbles by a microfluidic device and characterised by a nanoparticle tracking technique.[15] These independent studies provide a sufficient body of evidence to corroborate the existence of bulk nanobubbles.

However, it seems that nanobubbles have only been reported in water. Surface nanobubbles were reportedly observed in pure alcohols, but such observations have never been reproduced.[16] Häbich et al.[17] observed that mixtures of water-organic solvents scattered light for a long period of time (days) after mixing, which is consistent with the formation of nanoscale objects, but they attributed their observation to water-insoluble impurities in the organic solvents. Water is a very special liquid having a high surface tension and a structure composed of a network of hydrogen bonds, which allows water molecules to form complex structures around contaminants and may also allow water to support a strong surface charge. Such considerations might suggest that nanobubbles are perhaps specific to water.

In this paper, for the first time, we investigate the generation of bulk nanobubbles in an extensive range of aqueous organic solvent mixtures using acoustic cavitation. The nanobubble suspensions are visualised and characterised by a nanoparticle tracking analysis technique (NTA), and their surface charge is measured in terms of zeta potential. We monitor the nanobubble suspensions over a period of a few months and shed light on: (i) the different reasons behind the long-term stability of bulk nanobubbles in pure water versus their long-term stability in aqueous organic solvent solutions; and (ii) the reasons why bulk nanobubbles cannot exist in pure organic solvents and why they disappear at some organic solvent-water ratio.

Experimental methods

Materials

Analytical grade (99.5% pure) ethanol, methanol, 2-propanol and acetone were purchased from Fisher Scientific (UK) and were handled in a glassware in order to avoid contamination from plastic products. Ultrapure water from a Millipore purification system (Millipore-Q, UK) was used in all experiments. The electrical conductivity and pH of the purified water were 1.70 $\mu S.cm^{-1}$ and 6.7, respectively, at a temperature of 20.0 ˚C. Prior to experimentation, purified water and all solvents were examined for any nanoscale impurities using an NTA instrument, and no detectable amounts of nanoscale entities could be observed. The NTA instrument which was also used to determine the nanobubble count and measure the nanobubble size distribution is described further below.

Acoustic generation of bulk nanobubbles

Bulk nanobubbles were generated by ultrasound cavitation using a 20 kHz probe-type ultrasound processor (Autotune-Series 750W Model, Sonics & Materials). A titanium probe of 0.75-inch diameter was used to irradiate 80 mL of water-organic mixture inside a glass beaker, as shown in Fig. 1. The temperature of the sample was controlled at 20.0 ˚C by using a recirculating cooler (Julabo GmbH, Germany). In all experiments, the sonication time used was 180 s, corresponding to an ultrasound power input of approximately 52.7 W. After sonication, the nanobubble suspension was stored in 20 mL air-tight glass vials for further analysis of size distribution, number density, zeta potential and for monitoring of long-term stability of the nanobubbles.

Nanobubble number density and size distribution

The bubble size distribution was characterised using a NanoSight LM10 instrument (Malvern Instruments, UK). A Marlin CCD camera mounted on the microscope and operating at 30 frames per second, captures a video file of particles moving under Brownian motion. Nanoparticles or nanobubbles are, thus, indirectly tracked and their Brownian motion is analysed in real time, giving the bubble size distribution, mean bubble diameter and bubble number density. Each sample was

measured five times, each measurement lasting 90 s which is sufficient compared to the much shorter time scale of Brownian diffusion of nanoscale entities. The number of particles per frame varied from 10 to 170 depending on the nanobubble number density. A sample video sequence is provided for illustration in the Supporting Information-I. Prior to NTA measurements, the visualisation cell was first rinsed with pure water and dried with dry Nitrogen gas. This was further washed using a 10% propanol solution and again flushed with pure water and dried with dry Nitrogen gas.

We recently reported a comparison of the NTA and dynamic laser scattering (DLS) techniques, and showed that NTA is more reliable for the analysis of bulk nanobubbles (and nanoparticles) as DLS measurements tend to be biased towards large bubble sizes.[14] Furthermore, current DLS instruments do not measure the bubble number density. Since NTA can simultaneously analyse a population of nanoparticles on an individual basis, it is ideally suited for real-time analysis of polydisperse systems ranging from 10 to 2000 nm in size and 10^7 to 10^9 particles.mL^{-1} in particle number density.[19]

Zeta Potential

The electro-kinetic or zeta potential is a key indicator in the stability of a colloidal dispersion. Considering a suspended colloidal particle, the zeta potential is the electric potential in the interfacial double layer at the location of the slipping/shear plane relative to a point in the bulk fluid away from the interface.[20] In other words, zeta potential is the potential difference between the dispersion medium and the stationary layer of fluid attached to the dispersed colloidal particle. Zeta potential cannot be measured directly, but it can be derived using a theoretical model and an experimentally-determined electrophoretic mobility of charged entities under an applied electric field. The electrophoretic mobility, μ_e, is defined as:

$$\mu_e = \frac{u}{E} \tag{1}$$

where u is the drift velocity of the dispersed particle, and E is the strength of the applied electric field. Thus, the zeta potential, ζ, can be calculated from:[20]

$$\mu_e = \frac{2\varepsilon_r \varepsilon_0 \zeta f(\kappa a)}{3\eta} \tag{2}$$

where ε_r, ε_0, η, and $f(\kappa a)$ are, respectively, the relative permittivity or dielectric constant of the dispersion medium, the permittivity of vacuum, the dynamic viscosity of the dispersion medium at the experimental temperature and Henry's function which describes the electrophoretic mobility of a spherical colloidal particle in the limit of low surface potentials. In this study, the zeta potential of the

nanobubble suspensions was measured by a ZEN5600 ZetaSizer Nano ZSP (Malvern Instruments, UK). The Smoluchowski approximation[20] was used to estimate $f(\kappa a)$ as 1.5 for aqueous ethanol solutions. The values of refractive index and viscosity of the different ethanol-water mixtures were obtained from the literature.[21,22]

Results and discussion

Fig. 2(a) shows typical bulk nanobubble size distributions in pure water and in ethanol-water mixtures. With the addition of small amounts of ethanol, the nanobubble population produced in water-ethanol is many folds larger than that obtained in pure water. The mode of the distribution increases with increasing ethanol content up to a volume fraction of 20%, decreasing thereafter with no nanobubbles detected in the mixtures containing more than 70% ethanol. A close scrutiny of the bubble size distributions reveals that the mode shifts to the right as the volume fraction of ethanol increases. This trend is even more evident in the cumulative bubble size distributions shown in Fig. 2(b), where the slope of the cumulative curves clearly decreases with increasing volume fraction of ethanol, indicating that the number mean bubble size (d_{10}) increases monotonically and substantially with ethanol concentration, as depicted in Fig. 2(c).

The number density of nanobubbles is a more convenient parameter to compare nanobubble populations generated in different ethanol-water mixtures. As shown in Fig. 2(d), the bubble number density rises sharply to a maximum value of $\sim 2.8\times10^9$ bubble/mL as the ethanol volume fraction increases to 20%, and falls off sharply at higher ethanol fractions reaching zero bubble/mL at 70% ethanol. A similar trend was observed for other organic solvents. The number of nanobubbles in the suspensions generated was a maximum at a solvent concentration of about 50% for methanol, 20% for acetone and 10% for 2-propanol, as shown in Fig. 3.

The generation of bulk nanobubbles in water-solvent mixtures raises a number of key fundamental questions: (i) why is it possible to generate much larger populations of bulk nanobubbles in the presence of moderate amounts of an organic solvent (e.g., ethanol, methanol, acetone and 2-propanol) compared to pure water? (ii) why does the number density of nanobubbles generated reach a maximum at between 10-50% of solvent content? (iii) why does the mean nanobubble diameter increase with the volume fraction of organic solvent? (iv) why is it not possible to form nanobubbles in pure organic solvents?

Before attempting to answer these questions, it is important to shed some light on the formation of and stability of bulk nanobubbles in pure water. Nanobubbles generated in pure water have been reported to exhibit long-term stability on the order of several weeks[1-3]. A number of various theories have been proposed to explain such extraordinary longevity.[23] However, reports are sparse, and in the

main conflicting and have not been independently validated, so that here is no universally accepted theory that explains the existence and stability of bulk nanobubbles. Most interesting perhaps is the ion-stabilized model proposed by Bunkin et al.[24]. It conjectures that the presence of a negative electrostatic pressure due to adsorption of OH^- ions in the form of an electric double layer at the nanobubble interface, akin to that observed around solid nanoparticles, balances the internal Laplace pressure and, therefore, no net diffusion of gas occurs.

As discussed above, the zeta potential is a widely used measure of the magnitude of the surface charge of small dispersed entities, and the values measured for the nanobubble suspensions generated in the ethanol-water mixtures are presented in Fig. 4. The zeta potential decreases sharply with the volume fraction of ethanol from a maximum value of -31 mV in pure water to about -2 mV in the presence of 50% ethanol. This may be attributed to ethanol molecules adsorbing on the surface of the nanobubbles via hydrogen bonding and this is reflected in the zeta potential of the nanobubbles. Typical data on the long-term stability of nanobubbles in pure water and in ethanol-water mixtures are presented in Fig. 5, where the bubble size distribution of each nanobubble suspension was monitored over a long period of time. Thus, most of the nanobubbles were still stable after 3 months both in pure water as well as in the ethanol-water mixtures.

The adsorption of ethanol (or other solvent) molecules on the nanobubble interface may be explained by referring to the literature describing a planer aqueous ethanol-gas interface. Li et al.[25] used the Neutron and X-ray grazing incidence reflection method to characterize such an interface. They concluded that there is an ethanol (C_2H_5OH) layer at the interface with the ethyl group (C_2H_5) oriented towards the gas phase and the hydroxyl group (OH) oriented towards the liquid phase. This was independently confirmed by Taylor and Garett,[26] Tarek et al.[27] and Stewart et al.[28] via molecular dynamic simulations. Since the ethyl group is oriented towards the gas phase then the extent of hydrogen bonding near the interface is expected to be higher than in the bulk of the solution. This would be expected to result in both a strong O–H···O hydrogen bond and a weak C–H···O hydrogen bond in the vicinity of the interface, which was also confirmed by Tarek et al.[29] and Chen et al.[30] via molecular dynamic simulations. In the case of organic solvents, the strength of hydrogen bonds lies between 10 and 40 kJ.mol^{-1} or approximately 5 – 10 k_BT per bond at 298 K (where k_B is Boltzmann's constant and T is temperature), which is much stronger than a typical van der Waals bond ($\sim$ 1 kJ.mol^{-1}or $\sim$ 1 k_BT).[20] The presence of a strong hydrogen bond near the interface may be responsible for the stability of the bulk nanobubbles in organic solvent-water mixtures.

Now let us try to answer the first key question as to why the concentration of nanobubbles becomes maximum at between 10-50% of organic solvent. Gas oversaturation is a more appropriate parameter in determining the population of the bubbles.[4] If we assume that a pure organic solvent would act as a

gas sink removing any excess gas from the solution, then it would not form nanobubbles. Hence, if nanobubbles exist in pure water, then they should disappear at some organic solvent-water ratio. The solubility of atmospheric gases (Co_2, N_2) in water has been observed to be lower than the water-alcohol mixtures and, therefore, gas oversaturation is expected to be higher, when the alcohol content is 10-50% (v/v) [31,32], thus, resulting here in a maximum number density of nanobubbles.

Another interesting aspect concerns the composition of the gas inside the bulk nanobubbles which might be expected to consist mainly of non-condensable dissolved air and possibly some condensable water and solvent volatile vapour formed during ultrasound cavitation.[33] Since, as shown by the above results, bulk nanobubbles become increasingly more difficult to produce beyond a certain solvent volume fraction, this suggests that solvent vapour is in fact not necessary for bulk nanobubble formation and such nanobubbles must be filled with dissolved air released from the solution.

Furthermore, the number density and mean diameter of the nanobubbles formed using the various organic solvents investigated are compared in Fig. 6 for 20% solvent-water mixtures - comparison at all other volume fractions of the solvents investigated was consistent with the observations made for the 20% solvent-mixtures. The number density of nanobubbles is lowest in the methanol-water mixture and it is highest in the acetone-water mixture. This difference in behaviour may be attributed to the difference in gas oversaturation between the different organic solvents in water. Methanol has the highest solubility[34] and therefore expected to have lowest gas oversaturation and, in consequence, the nanobubble count per volume is found to be the lowest (Fig. 6). All the other solvents follow the same trend as a function of their solubility in water.

It is well known that the solubility of atmospheric gases in aqueous organic solvent solutions improves at lower temperatures[31,32,34]. Thus, cooling of the suspensions should lead to a significant increase in gas oversaturation and an increase in the nanobubble number density should, therefore, be expected. In order to test this hypothesis further, freezing and thawing experiments of the bulk nanobubble suspensions were conducted. Thus, 20 mL samples of nanobubble suspensions in pure water and in mixtures of water and organic solvent were kept in air-tight glass vials in different freezers at temperatures of -18 ˚C and -80 ˚C for a period of 24 hours. Subsequently, these samples were withdrawn from the freezers and left to thaw at room temperature for about 6 hours before being analysed by the NTA technique. Furthermore, given that water-ethanol solutions have different freezing points depending on the ethanol concentration, in order to ensure that all of the ethanol in the mixture had frozen, freezing experiments were also conducted by dipping nanobubble suspensions in liquid Nitrogen at -180 ˚C.

Representative results are presented in Fig. 7, showing bubble size distributions for suspensions in pure water and 20% ethanol in water. After thawing of the samples, the nanobubbles formed in pure water vanished virtually completely. Ohgaki et al.[2] and Ebina et al.[3] showed using ESEM that frozen nanobubble suspensions consisted of spherical cavities of about 100 nm diameter. This suggests that nanobubbles are not destroyed during freezing but rather during thawing. The freeze-thaw process of nanobubble suspensions consists of a number of transformations which may individually or collectively cause the collapse of the nanobubbles. Thawing leads to a complex rearrangement of molecules and it is slower than the freezing process as ice is a poor conductor of heat. During thawing, the kinetic energy of molecules increases. This, in turns, leads to a random motion of the molecules as transition occurs from the solid to the liquid state. It is also possible that during freezing nanobubble interfaces in distilled water could also freeze and subsequently collapse due to molecular rearrangement on thawing. It should also be noted that the gas pressure inside a nanobubble will reduce significantly as the temperature is lowered which might also cause subsequent collapse of the bubble interfaces upon thawing.

However, the nanobubble suspension produced in the 20% ethanol-water mixture behaved strikingly differently. There was practically no change in the bubble size distribution after individual samples were frozen at -18 ˚C, -80 ˚C and -180 ^{0}C and thawed. Whilst there was no significant change in bubble number density in the sample which was frozen at -18 ˚C, the samples frozen at -80 ˚C and -180 ˚C exhibited an increase of 3 folds in the bubble number density. These ethanol-water nanobubble suspensions were analysed again after seven days and the distributions were practically unchanged (Fig. 7). Unlike in pure water, we presume that ethanol molecules, as illustrated in Fig 8, attach to the interface of nanobubbles via hydrogen bonding providing a thick protective shell that shields the nanobubbles, which prevents them from disappearing on thawing. The increase in bubble number density was more pronounced at lower ethanol contents below 20%, but the effects reduced at ethanol concentrations above 20% and disappeared at 50% (see Fig. 9). Similar findings were obtained for the other solvents.

As expected, cooling of the ethanol-water suspensions causes a significant increase in air supersaturation as the solubility decreases with temperature.[31,32] During the process of thawing, the sample heats up, its temperature rises and the solubility of air in the water-solvent mixture reduces. Consequently, dissolved air is spontaneously released from both water and liquid solvent and, hence, the population of nanobubbles increases. This effect, however, is only noticed at -80 ˚C and -180 ˚C but not at -18 ˚C. This may be due to the degree of supersaturation being much higher at -80 ˚C and -180 ˚C than at -18 ˚C. The same effects on bubble number density occurred to different extents at various volume fractions and in all the other solvent-water mixtures investigated, as illustrated by typical data in Fig. 9.

Now the other key question is why no nanobubbles can be generated in pure organic solvents. There are two possible interpretations: (i) nanobubbles can be generated in pure organic solvents but they are not stable and quickly dissolve; or (ii) nanobubbles cannot be generated in a pure organic solvent. Given the high solubility of atmospheric gases in organic solvents,[31] it is difficult to envisage that nanobubbles cannot be formed at all. As discussed above, the stability of nanobubbles in pure water is attributed to the presence of a significant charge afforded by the selective adsorption of hydroxyl ions on the interface. Whilst hydroxyl ions are present in water because of self-ionisation, this is not the case in organic solvents which do not autoionise. Such a surface charge is deemed essential for the stability of nanobubbles in water. We support the plausible proposition that the adsorption of hydroxyl ions in the form of an electric double layer at the nanobubble interface creates an external electrostatic pressure, which balances the internal Laplace pressure and, therefore, prevents gas diffusion at equilibrium. However, the mechanism of stabilisation seems to be different in aqueous mixtures of organic solvents. In fact, results shown in Fig. 5 confirm that nanobubbles with a weak zeta potential are still stable in aqueous organic solutions (over 3 months). A typical Fast Field Reversal (FFR) and Slow Field Reversal (SFR) plot is provided in Fig. S1 (see Supporting Information-II) to demonstrate the accuracy of such low zeta potential measurements.

Macro and microbubbles formed in aqueous surfactant solutions have been reported to reduce in size as surface tension is lowered.[35-37] However, the diameter of nanobubbles generated in the aqueous organic solvent mixtures investigated here, increases approximately linearly with solvent volume fraction whilst in fact surface tension reduces considerably, e.g. from 0.073 $N.m^{-1}$ down to 0.023 $N.m^{-1}$ for ethanol-water solutions[38] (see Fig. 10). Macro and microbubbles in aqueous organic solutions (e.g. methanol, ethanol, 1-propanol, 2-propanol) have also been reported to behave in a similar manner.[39,40] This paradox, however, remains unexplained. A possible explanation might be that organic solvents do not behave like surface active agents; they reduce surface tension by dilution of bulk water but their molecules do not adsorb at the gas-liquid interface. In a surfactant solution, as surface tension reduces the initial bubble size generated is reduced. Whilst a surfactant hinders coalescence via slow liquid film thinning between approaching bubble interfaces which are loaded with surfactant molecules, this does not happen in case of a water-organic mixture and bubble coalescence occurs more readily leading to larger bubbles.

Conclusions

The formation of bulk nanobubble suspensions using an acoustic cavitation technique and their stability have been studied in various aqueous organic solvent mixtures (ethanol, acetone, methanol, 2-propanol). Nanobubbles generated in pure water and in water-organic mixture enjoy long-term stability with most of them surviving after more than 3 months. The addition of small amounts of

solvent to pure water increases the nanobubble population generated by cavitation several folds. This trend increases sharply with solvent content, reaching a maximum at an intermediate solvent concentration, generally around 10%-50%. This behaviour is attributed to the gas oversaturation of water which is expected to be maximum in mixtures containing about 10-50% of organic solvent. Freezing and thawing experiments of the nanobubble suspensions corroborate the hypothesis as the nanobubble count further increases upon defrosting of the nanobubble samples. Beyond this maximum, the bubble number density falls off sharply with no nanobubbles forming when the solvent content is higher than a certain value, generally around 60-70%. A pure organic solvent acts as a gas sink removing any excess gas from the solution and thus does not form nanobubbles. Hence, nanobubbles in pure water disappear at some organic solvent-water ratio depending on the type of solvent. The stability of nanobubbles in pure water is attributed to the presence of a significant charge afforded by the adsorption of hydroxyl ions on the interface. Whilst hydroxyl ions are present in water because of self-ionisation, this is not the case in pure organic solvents which do not auto-ionise and, therefore, nanobubbles cannot exist in concentrated aqueous organic solvent solutions. Due to preferential adsorption of organic solvent molecules at the nanobubble interfaces, the surface charge of the nanobubbles decreases with solvent content, but the strong hydrogen bonding near their interfaces ensures their stability. The mean bubble size increases monotonically with solvent content whilst surface tension is sharply reduced, in agreement with literature results on macro and microbubbles in aqueous organic solutions. This result stands in stark contrast to the behaviour of macro and microbubbles in aqueous surfactant solutions.

Acknowledgements

This work was supported by EPSRC Grant EP/L025108/1. The loan of a Zetasizer Nano ZSP by Malvern Instruments (UK) is gratefully acknowledged.

Supporting Information

A sample video sequence of bulk nanobubbles in a water-ethanol system is presented in Supporting Information-I; and a typical Fast Field Reversal (FFR) and Slow Field Reversal (SFR) plot is shown in Fig. S1 in Supporting Information-II.

References

(1) Weijs, J. H.; Seddon, J. R. T.; Lohse, D. Diffusive shielding stabilizes bulk nanobubble clusters. *ChemPhysChem* **2012**, *13*, 2197-2204.

(2) Ohgaki, K.; Khanh, N. Q.; Joden, Y.; Tsuji, A.; Nakagawa, T. Physicochemical approach to nanobubble solutions. *Chem. Eng. Sci.* **2010,** *65*, 1296-1300.

(3) Ebina, K.; Shi, K.; Hirao, M.; Hashimoto, J.; Kawato, Y.; Kaneshiro, S.; Morimoto, T.; Koizumi, K.; Yoshikawa, H. Oxygen and air nanobubble water solution promote the growth of plants, fishes, and mice. *PLoS ONE* **2013**, *8* 1-7.

(4) Epstein, P. S.; Plesset, M. S. On the stability of gas bubbles in liquid-gas solutions. *J. Chem. Phys* **1950**, *18*, 1505-1509.

(5) Liu, H.; Cao, G. Effectiveness of the Young-Laplace equation at nanoscale. *Scientific Reports* **2016,** *6*, 23936.
(6) German, S. R.; Edwards, M. A.; Chen, Q.; White, H. S. Laplace Pressure of Individual H2 Nanobubbles from Pressure–Addition Electrochemistry. *Nano Letters* **2016,** *16* (10), 6691-6694.
(7) Alheshibri M.; Craig, V. In *The puzzling existence of nanobubbles in aqueous solution*, 8th Biennial Australian Colloid & Interface, Coffs Harbour, Australia, Jan 29-Feb 2, 2017.
(8) Sedlák, M.; Rak, D. Large-scale inhomogeneities in solutions of low molar mass compounds and mixtures of liquids: Supramolecular structures or nanobubbles? *J. Phys. Chem. B* **2013,** *117*, 2495-2504.
(9) Jin, F.; Ye, J.; Hong, L.; Lamb, H.; Wu ,C. Slow relaxation mode in mixtures of water and organic molecules: Supramolecular structures or nanobubbles? *J. Phys. Chem. B* **2007**, *111*, 2255-2261.
(10) Leroy, V.; Norisuye, T. Investigating the Existence of Bulk Nanobubbles with Ultrasound. *ChemPhysChem* **2016,** *17* (18), 2787-2790.
(11) Uchida, T.; Oshita, S.; Ohmori, M.; Tsuno, T.; Soejima, K.; Shinozaki, S.; Take, Y.; Mitsuda, K. Transmission electron microscopic observations of nanobubbles and their capture of impurities in wastewater. *Nanoscale Res. Lett.* **2011,** *6*, 295-295.
(12) Li, M.; Tonggu, L.; Zhan, X.; Mega, T. L.; Wang, L. Cryo-EM Visualization of Nanobubbles in Aqueous Solutions. *Langmuir* **2016,** *32*, 11111-11115.
(13) Bunkin, N.; Shkirin, A.; Ignatiev, P.; Chaikov, L.; Burkhanov, I.; Starosvetskij, A. Nanobubble clusters of dissolved gas in aqueous solutions of electrolyte. I. Experimental proof. *J. Chem. Phys.* **2012,** *137* (5), 054706.
(14) Nirmalkar, N.; Pacek, A. W.; Barigou, M. On the Existence and Stability of Bulk Nanobubbles. *Langmuir* **2018,** *34* (37), 10964-10973.
(15) Nirmalkar, N.; Pacek, A.; Barigou, M. Interpreting the interfacial and Colloidal Stability of Bulk Nanobubbles. *Soft Matter* **2018,** DOI:10.1039/C8SM01949E.
(16) Simonsen, A. C.; Hansen, P. L.; Klösgen, B. Nanobubbles give evidence of incomplete wetting at a hydrophobic interface. *J. Colloid Interf. Sci*. **2004,** *273* (1), 291-299.
(17) Häbich, A.; Ducker, W.; Dunstan, D. E.; Zhang, X. Do stable nanobubbles exist in mixtures of organic solvents and water? *J. Phys. Chem. B* **2010,** *114* (20), 6962-6967.
(18) Sutherland, W.; Dynamical theory of diffusion for non-electrolytes and the molecular mass of albumin. *Phil. Mag.* **1905**, *9*, 781-785.
(19) NanoSight LM10. http://www.malvern.com/en/products/product-range/nanosight-range/nanosight-lm10/(accessed November l 9, 2018).
(20) Israelachvili, J. N. *Intermolecular and Surface Forces: With Applications to Colloidal and Biological Systems*; Academic Press, 1985.
(21) Scott, T. A. Refractive Index of Ethanol–Water Mixtures and Density and Refractive Index of Ethanol–Water–Ethyl Ether Mixtures. *The Journal of Physical Chemistry* **1946,** *50* (5), 406-412.
(22) Yusa, M.; Mathur, G. P.; Stager, R. A. Viscosity and compression of ethanol-water mixtures for pressures up to 40,000 psig. *Journal of Chemical & Engineering Data* **1977,** *22* (1), 32-35.
(23) Yasui, K.; Tuziuti, T.; Kanematsu, W.; Kato, K. Dynamic Equilibrium Model for a Bulk Nanobubble and a Microbubble Partly Covered with Hydrophobic Material. *Langmuir* **2016,** *32* (43), 11101-11110.
(24) Bunkin, N. F.; Shkirin, A. V.; Suyazov, N. V.; Babenko, V. A.; Sychev, A. A.; Penkov, N. V.; Belosludtsev, K. N.; Gudkov, S. V. Formation and Dynamics of Ion-Stabilized Gas Nanobubble Phase in the Bulk of Aqueous NaCl Solutions. *J. Phys. Chem. B* **2016,** *120* (7), 1291-1303.
(25) Li, Z. X.; Lu, J. R.; Styrkas, D. A.; Thomas, R. K.; Rennie, A. R.; Penfold, J. The structure of the surface of ethanol/water mixtures. *Molecular Physics* **1993,** *80* (4), 925-939.
(26) Taylor, R. S.; Garrett, B. C. Accommodation of Alcohols by the Liquid/Vapor Interface of Water: Molecular Dynamics Study. *The Journal of Physical Chemistry B* **1999,** *103* (5), 844-851.
(27) Tarek, M.; Tobias, D. J.; Klein, M. L. Molecular dynamics investigation of an ethanol-water solution. *Physica A: Statistical Mechanics and its Applications* **1996,** *231* (1), 117-122.
(28) Stewart, E.; Shields, R. L.; Taylor, R. S. Molecular Dynamics Simulations of the Liquid/Vapor Interface of Aqueous Ethanol Solutions as a Function of Concentration. *The Journal of Physical Chemistry B* **2003,** *107* (10), 2333-2343.
(29) Tarek, M.; Tobias, D. J.; Klein, M. L. Molecular dynamics investigation of the surface/bulk equilibrium in an ethanol–water solution. *Journal of the Chemical Society, Faraday Transactions* **1996,** *92* (4), 559-563.

(30) Chen, B.; Siepmann, J. I.; Klein, M. L. Vapor−Liquid Interfacial Properties of Mutually Saturated Water/1-Butanol Solutions. *Journal of the American Chemical Society* **2002,** *124* (41), 12232-12237.
(31) Tokunaga, J. Solubilities of oxygen, nitrogen, and carbon dioxide in aqueous alcohol solutions. *Journal of Chemical & Engineering Data* **1975,** *20*, 41-46.
(32) Dalmolin, I.; Skovroinski, E.; Biasi, A.; Corazza, M. L.; Dariva, C.; Oliveira, J. V. Solubility of carbon dioxide in binary and ternary mixtures with ethanol and water. *Fluid Ph. Equilibria* **2006,** *245* (2), 193-200.
(33) Yasui, K. *Acoustic Cavitation and Bubble Dynamics*; Springer International Publishing, 2017.
(34) Katayama, T.; Nitta, T. Solubilities of hydrogen and nitrogen in alcohols and n-hexane. *Journal of Chemical & Engineering Data* **1976,** *21* (2), 194-196.
(35) Rodrigues, R. T.; Rubio, J. New basis for measuring the size distribution of bubbles. *Miner. Eng.* **2003,** *16* (8), 757-765.
(36) Parhizkar, M.; Edirisinghe, M.; Stride, E. The effect of surfactant type and concentration on the size and stability of microbubbles produced in a capillary embedded T-junction device. *RSC Adv.* **2015,** *5* (14), 10751-10762.
(37) Cho, S.-H.; Kim, J.-Y.; Chun, J.-H.; Kim, J.-D. Ultrasonic formation of nanobubbles and their zeta-potentials in aqueous electrolyte and surfactant solutions. *Colloids Surf. A* **2005,** *269* (1), 28-34.
(38) Vazquez, G.; Alvarez, E.; Navaza, J. M. Surface Tension of Alcohol Water + Water from 20 to 50 .degree.C. *J. Chem. Eng. Data* **1995,** *40* (3), 611-614.
(39) Hu, B.; Nienow, A. W.; Stitt, E. H.; Pacek, A. W. Bubble Sizes in Agitated Water−Hydrophilic Organic Solvents for Heterogeneous Catalytic Reactions. *Ind. Eng. Chem. Res.* **2007,** *46* (13), 4451-4458.
(40) Hu, B.; Nienow, A. W.; Hugh Stitt, E.; Pacek, A. W. Bubble sizes in agitated solvent/reactant mixtures used in heterogeneous catalytic hydrogenation of 2-butyne-1,4-diol. *Chem. Eng. Sci.* **2006,** *61* (20), 6765-6774.

Figure and Table captions

Fig. 1. Schematics of experimental set-up used to generate bulk nanobubbles.

Fig. 2. Bulk nanobubbles in ethanol-water mixtures: (a) bubble size distributions; (b) cumulative bubble size distributions; (c) mean bubble diameter; (d) bubble number density.

Fig. 3. Typical bubble size distributions in different water-organic systems: (a) methanol-water; (b) acetone-water; (c) 2-propanol-water; (d) effect of solvent volume fraction on bubble number density.

Fig. 4. Zeta potential of bulk nanobubble suspensions generated in ethanol-water mixtures.

Fig. 5. Long-term stability of bulk nanobubbles: (a) pure water; (b) 20% ethanol-water mixture.

Fig. 6. Bulk nanobubbles in 20% organic solvent-water mixture: (a) bubble number density; (b) mean bubble diameter.

Fig. 7. Freezing and thawing of bulk nanobubbles: (a) pure water; (b) 10% ethanol-water mixture; (c) 20% ethanol-water mixture; (d) 50% ethanol-water mixture.

Fig. 8. Schematics of formation of protective organic shell around nanobubbles in a water-alcohol system.

Fig. 9. Bubble size distribution before and after freezing and thawing of (a) 10% 2-propanol-water and (b) acetone-water mixture.

Fig. 10. Variation of mean bubble diameter and surface tension of ethanol-water mixtures.

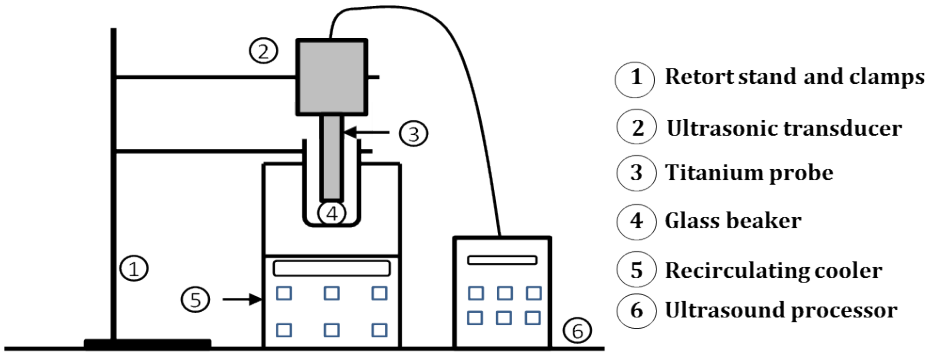

Fig. 1. Schematics of experimental set-up used to generate bulk nanobubbles.

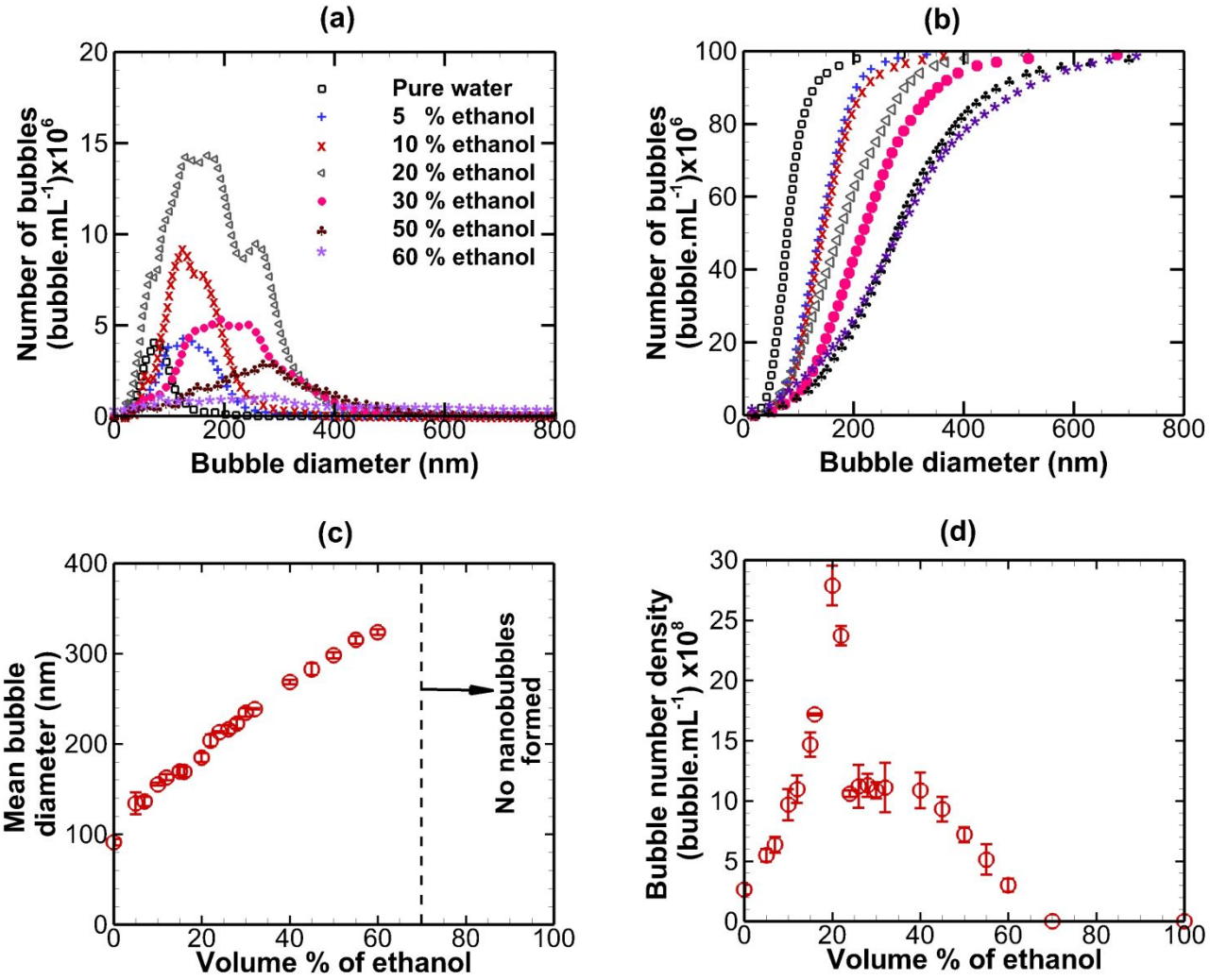

Fig. 2. Bulk nanobubbles in ethanol-water mixtures: (a) bubble size distributions; (b) cumulative bubble size distributions; (c) mean bubble diameter; (d) bubble number density.

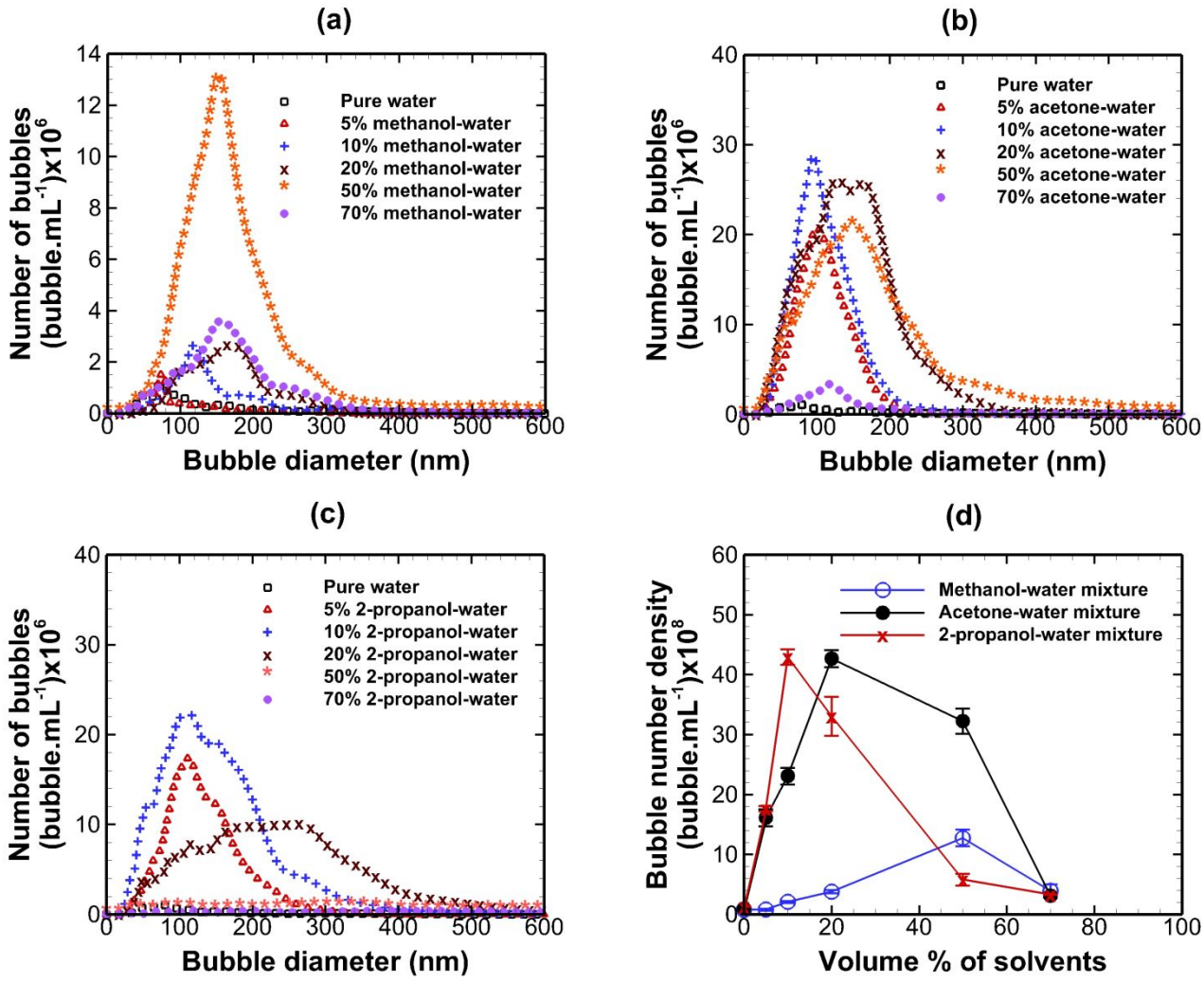

Fig. 3. Typical bubble size distributions in different water-organic systems: (a) methanol-water; (b) acetone-water; (c) 2-propanol-water; (d) effect of solvent volume fraction on bubble number density.

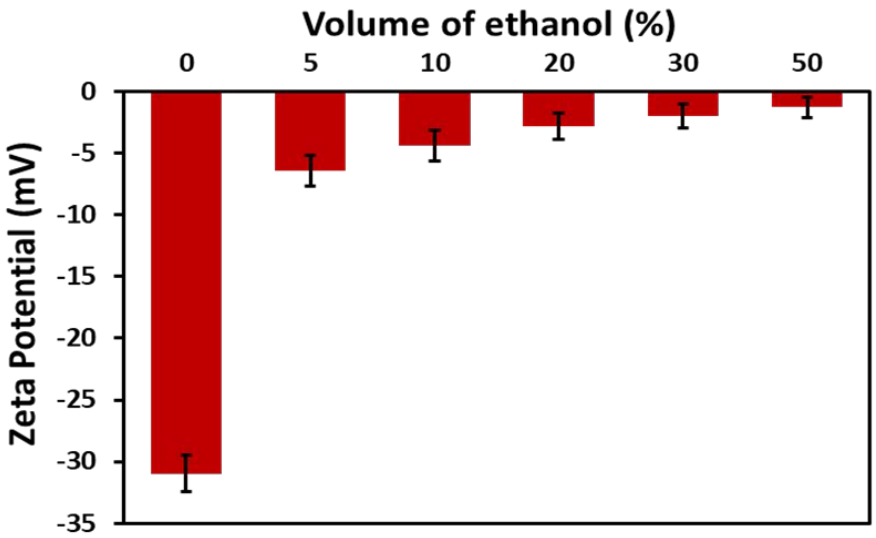

Fig. 4. Zeta potential of bulk nanobubble suspensions generated in ethanol-water mixtures.

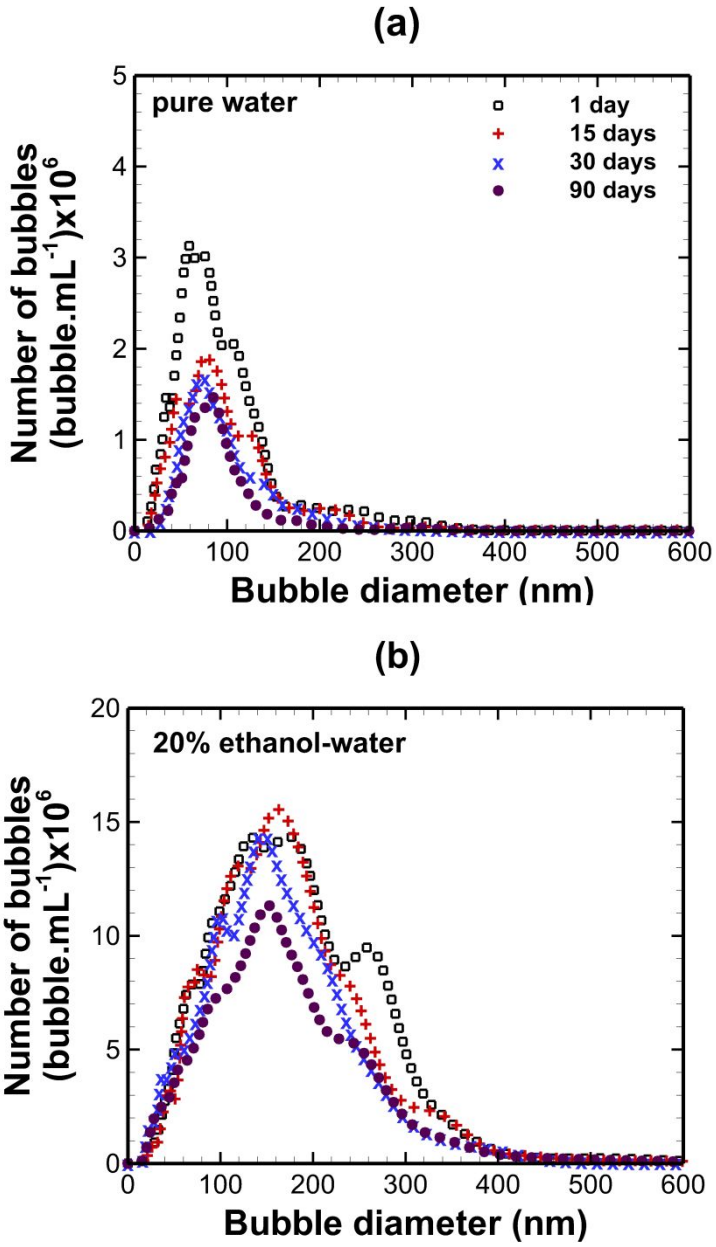

Fig. 5. Long-term stability of bulk nanobubbles: (a) pure water; (b) 20% ethanol-water mixture.

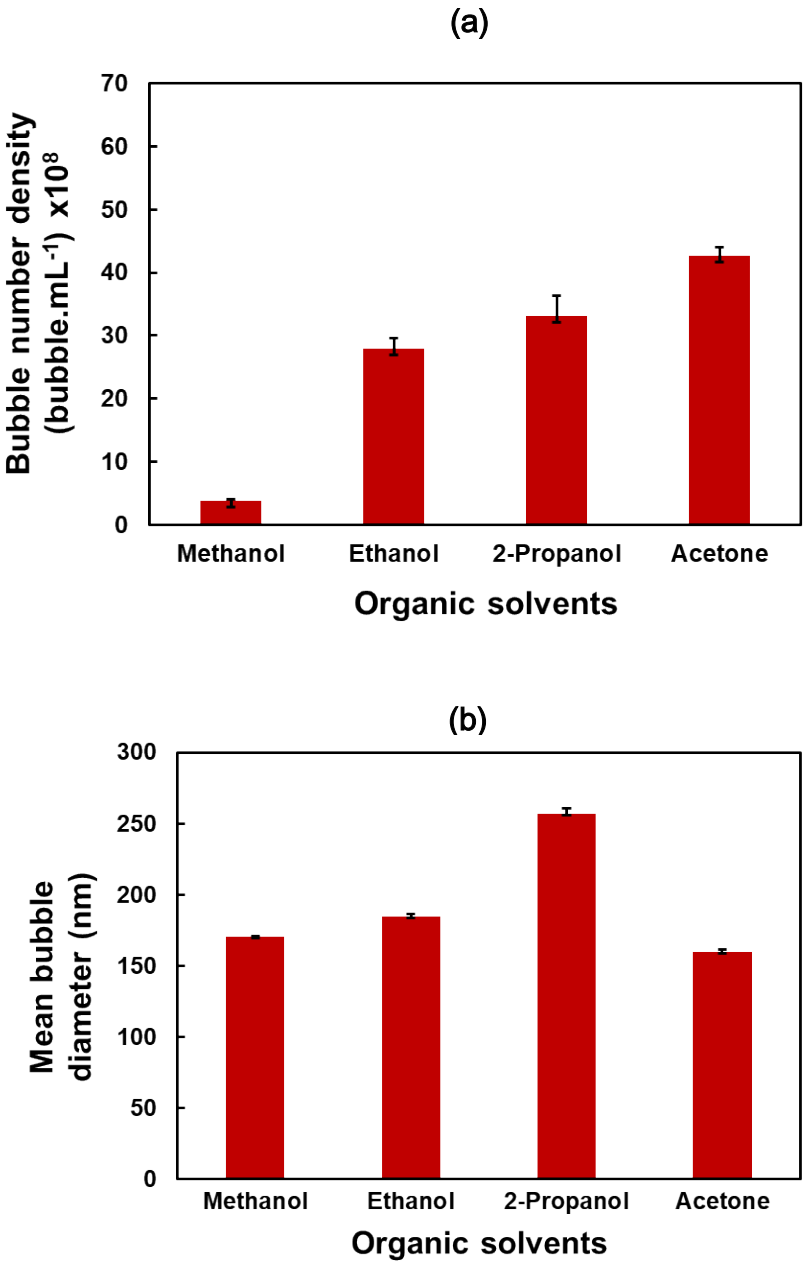

Fig. 6. Bulk nanobubbles in 20% organic solvent-water mixture: (a) bubble number density; (b) mean bubble diameter.

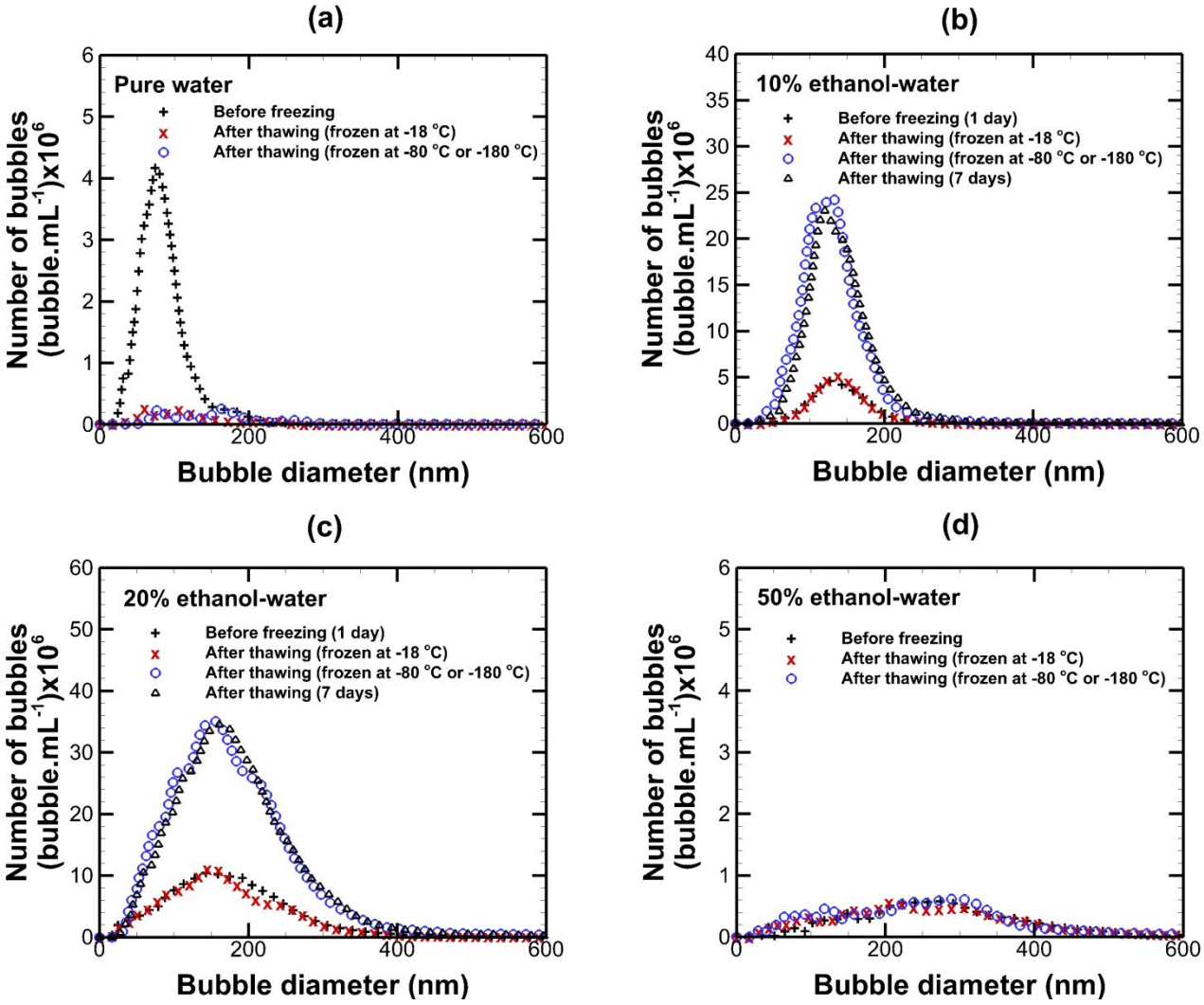

Fig. 7. Freezing and thawing of bulk nanobubbles: (a) pure water; (b) 10% ethanol-water mixture; (c) 20% ethanol-water mixture; (d) 50% ethanol-water mixture.

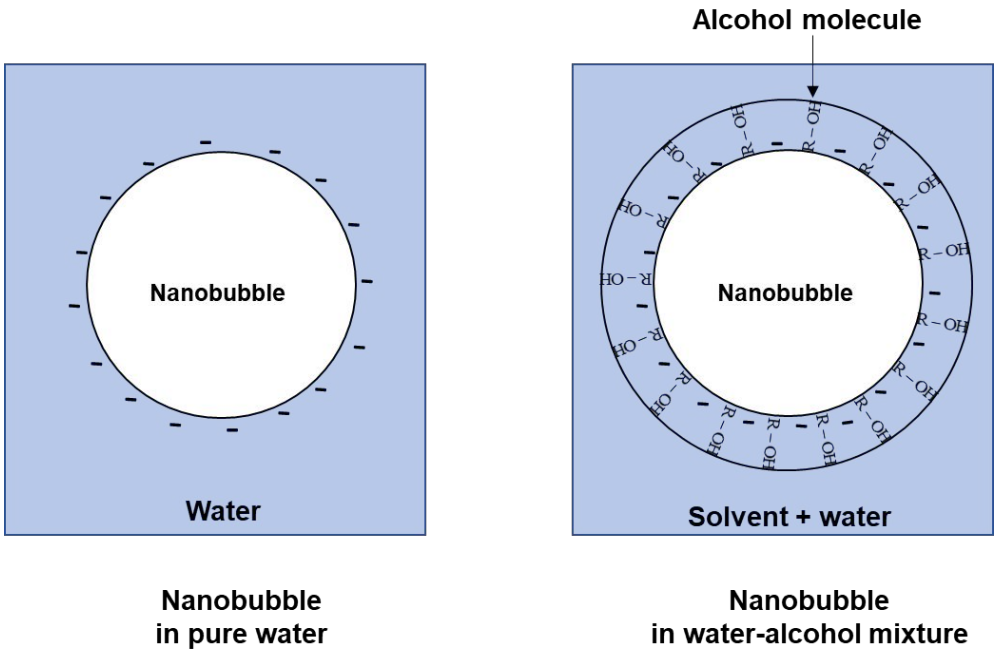

Fig. 8. Schematics of formation of protective organic shell around nanobubbles in a water-alcohol system.

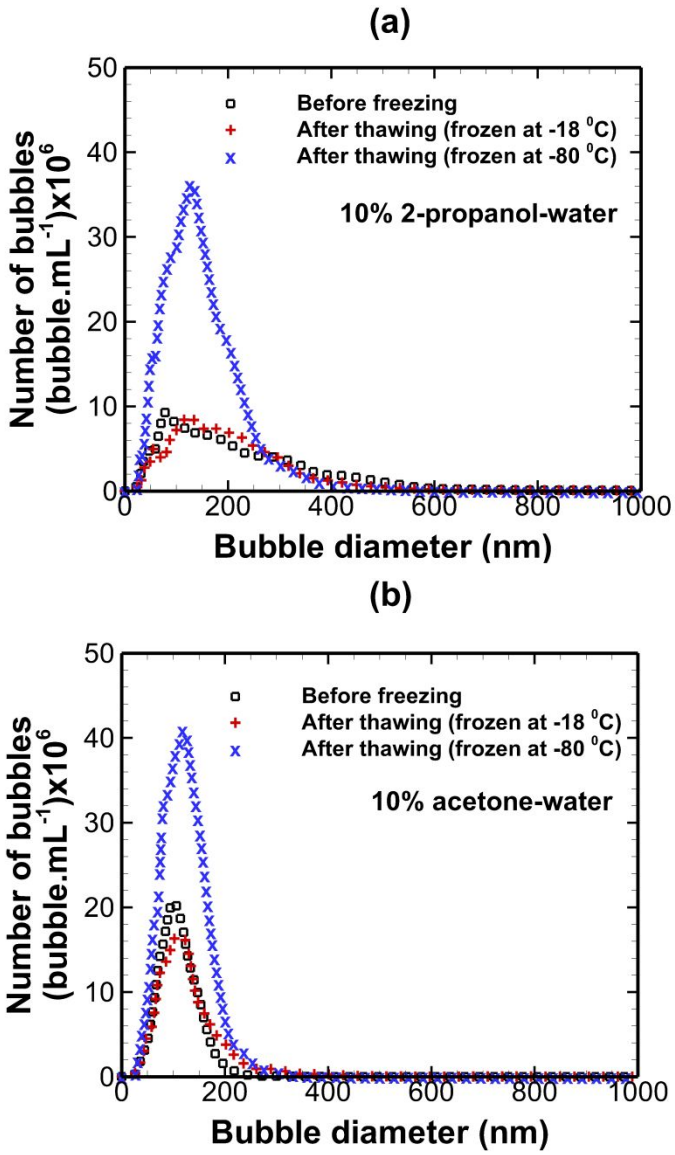

Fig. 9. Bubble size distribution before and after freezing and thawing of (a) 10% 2-propanol-water and (b) acetone-water mixture.

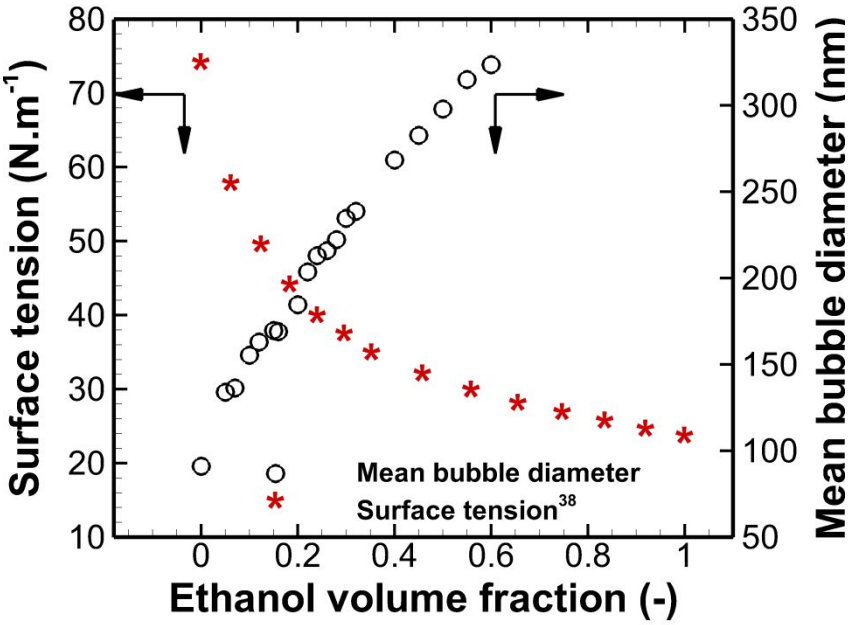

Fig. 10. Variation of mean bubble diameter and surface tension of ethanol-water mixtures.

Table of Contents Graphic